Original Article

Low-cost three-dimensional printed orbital template-assisted patient-specific implants for the correction of spherical orbital implant migration

Tarjani Vivek Dave[1,2], Sweety Tiple[1,2], Sandeep Vempati[3], Mansha Palo[1], Mohammad Javed Ali[2], Swathi Kaliki[2], Milind N Naik[2]

Purpose: To describe the outcomes of a patient-specific implant (PSI), fabricated using a three-dimensional (3D) printed orbital template and placed in the basin of the inferior orbital fissure to correct inferotemporally migrated spherical orbital implant. **Methods:** This is a single-center, prospective, consecutive, interventional, case series of six patients, with non-porous, spherical, orbital implant migration that underwent implant recentration surgically with a novel technique. Migration was subclassified either as decentration that did not affect the prosthetic retention or as displacement that affected the prosthetic retention in the eye socket. Only implant displacements were treated. The primary outcome measure was centration of the implant clinically and radiologically, with ability to retain the prosthesis. **Results:** At a mean follow-up of 21 months, all six orbital spherical implants remained centered. There were no cases of extrusion, exposure, or migration of either implants. There were no cases of PSI displacement. Additional procedures to optimize the aesthetic outcome of the customized ocular prosthesis (COP) required were simultaneous fornix formation suture in three patients, subsequent fornix formation with mucus membrane graft in two patients, and levator resection and sulcus hyaluronic acid gel injection in one patient each. The mean PSI implant weight was 2.66 ± 0.53 g. The mean COP weight was 2.2 ± 0.88 g postoperatively. The median patient satisfaction with the procedure was 9 on 10. **Conclusion:** A 3D printing-assisted PSI placed in the basin of the inferior orbital fissure allows recentration of the migrated implant over a follow-up of 21 months without complications.

Access this article online

Website: www.ijo.in

DOI: 10.4103/ijo.IJO_472_18

Quick Response Code:

Key words: Anophthalmic socket, complication, implant migration, orbital implant, three-dimensional printing

Evisceration and enucleation with implant are commonly performed oculoplastic procedures. While the surgery itself is not very challenging, the management of implant-related complications often is. Mechanisms for orbital implant exposure and extrusion and the rates of these complications have been extensively reported in literature.[1-3] However, implant migration has been sparsely addressed. Migration is seen more frequently in patients with non-porous implants since these are devoid of fibrovascular tissue ingrowth that holds the implant in position[1] and in hydrogel orbital implants used for orbital volume expansion in congenital anophthalmia and microphthalmia.[4] Furthermore, the rate of migration is higher when the implant placement is performed as a secondary procedure.[5] When the migrated orbital implant affects prosthesis placement and centration, surgical correction of migration is required. Treatment options include implant exchange and dermis fat graft (DFG).[5-7] Both these options come along with the associated complications such as re-migration of the implant after implant exchange and graft necrosis after DFG, especially in previously operated sockets. Lack of scientific evidence and a limited understanding of the pathophysiologic basis of implant migration led us to look at an alternative approach in its management.

[1]Socket, Anophthalmia and Orbito-facial Prosthesis Service, [2]Ophthalmic Plastic Surgery Service, [3]Srujana Center for Innovation, LV Prasad Eye Institute, Hyderabad, Telangana, India

Correspondence to: Dr. Tarjani Vivek Dave, LV Prasad Eye Institute, Road No 2, Banjara Hills, Hyderabad - 500 034, Telangana, India. E-mail: tvdeye@gmail.com

Manuscript received: 01.04.18; Revision accepted: 13.07.18

Following an initial report of successful three-dimensional (3D) printing-aided fabrication of patient-specific implant (PSI) in the management of implant migration,[8] we describe the outcomes as novel, cost-effective, minimally invasive, and a lasting technique of 3D printing-aided PSIs in the management of inferotemporal spherical orbital implant migration.

Methods

Study approval, design, and subjects

This is a single-center, prospective, consecutive, case series including six patients with prior socket surgery presenting with inferotemporal implant migration. Institutional Review Board/Ethics Committee approval was obtained. All patients presenting to the Ophthalmic Plastic Surgery Service or the Ocular Prosthesis Laboratory from January 2014 to December 2016 with inferotemporal implant migration were included. Migration was classified as decentration and displacement based on our previous work.[9] All six patients had an

Cite this article as: Dave TV, Tiple S, Vempati S, Palo M, Ali MJ, Kaliki S, *et al*. Low-cost three-dimensional printed orbital template-assisted patient-specific implants for the correction of spherical orbital implant migration. Indian J Ophthalmol 2018;66:1600-7.

inferotemporal displacement of the implant with the implant palpable anterior to the inferior orbital rim and consequent shallowing of the inferior fornix. They had inability to retain a custom ocular prosthesis (COP) or achieve a satisfactory centration of the prosthesis after maximal prosthesis modification by an expert ocularist. Patients with decentration of the implant but deep fornices and patients with a shallow inferior fornix but central implant were excluded. All patients received a PSI, custom-designed with the aid of 3D printing the ipsilateral orbit and were operated by one faculty in the service (TVD). A COP was fabricated and dispensed after surgical interventions in all patients. Additional procedures required either along with the PSI placement or over the follow-up period were documented [Fig. 1].

Outcome measures

The primary outcome measure was the recentration of the migrated spherical implant clinically and radiologically and the ability to retain the prosthesis in the eye socket. The secondary outcome measures were the mean PSI weight and factors contributing to the implant and prosthesis correlation such as the mean implant diameter, pre- and postoperative thickness of the COP, pre- and postoperative weight of the COP, pre- and postoperative enophthalmos, pre- and postoperative superior sulcus deformity (SSD), and other postoperative complications. The weights of the prosthesis and the PSIs were measured on one constant weighing scale. The thickness of the COP was measured with one constant caliper. The SSD was graded from grade 0 to 4 as described earlier.[10] Patient satisfaction with the outcome of the procedure was scored on a visual analog scale in a linear fashion from 0 to 10 with 0 indicating least satisfaction and 10 indicating maximum satisfaction with the procedure.[11,12]

Data collection

The data collected included the demographic details, the indication for surgery and the past ocular procedures, computed tomography (CT) orbit with details of the spherical orbital implant, PSI fabrication details, the surgical technique, and the surgical steps. Socket examination findings preoperatively and over the available postoperative period visit included the (a) examination of the socket with the prosthesis, (b) examination of the socket without the prosthesis, and (c) the examination of the prosthesis. The pre- and postoperative CT scan was assessed for the position of the implants in the orbit. The postoperative complications were noted.

Surgical techniques

Three-dimensional printing details

DICOM images from the patients' CT scan were reconstructed as a 3D model, and the region of interest around the orbit with the primary migrated implant was segmented and exported as a binary STL file [Fig. 1]. This was imported into a STL modeling software known as CURA. The solid models were sliced into several two-dimensional layers using a 3D printing software. To build an accurate 3D model, support structures were generated to provide structural integrity. Distinct tool paths were generated for the model and the support structures in G-code (RS-247) format, using which models were then 3D printed in Ultimaker 2, an additive manufacturing system that uses fused deposition modeling. 3D printing was done at 200-μm layer thickness and with 20% infill and 1.2-mm layer thickness at a 40 mm/s print speed to get smooth surface features and rigidity. The model was 3D printed with polylactic acid for its ease of print and reliability. Once the 3D printed model was ready, the support structures were removed using needle nose pliers and polished with 800 grit sand paper.

Patient-specific implant fabrication

Using this skull model as a mould, a polymethyl methacrylate (PMMA) implant was fabricated to rest in the basin of the inferior orbital fissure. The 3D printed orbital model served as a mould to get an accurate impression of the

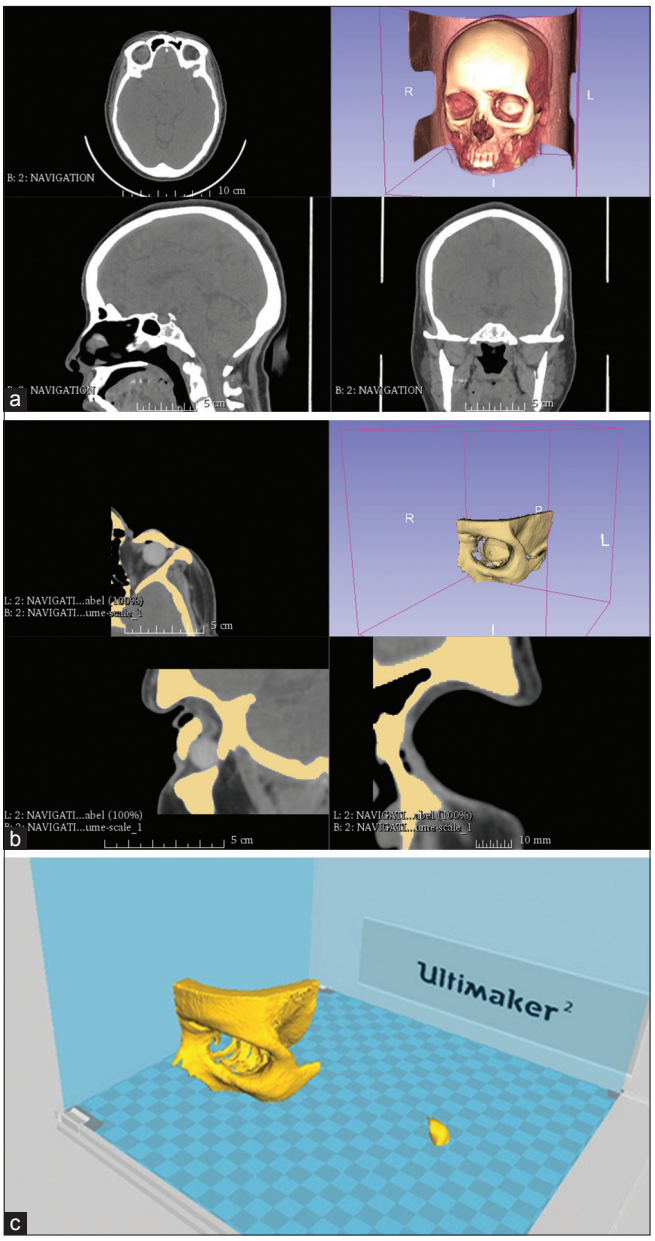

Figure 1: Conversion of the patient's computed tomography scan to a three-dimensional (3D) model. (a) Exporting the patient's two-dimensional computed tomography scans and converting it to a 3D model, (b) cropping the 3D model to the region of interest, in this case the left orbit, and (c) removing the implant from the orbit and exporting STL file to 3D printer

inferior surface or base of the PSI. The PSI was fabricated as a dome-shaped implant. The reason to consider 3D printing of the orbit was to get an accurate base shape and base dimension of the implant and also get a clue on what height the PSI needs to have to achieve optimal centration of the spherical implant as demonstrated in the picture below [Fig. 2]. The PSI was fabricated in four different heights starting with 10mm and reducing by a millimeter each to 7 mm as demonstarted in images d,f,h and i in Fig. 2. The PSI height giving the best centration of the spherical implant in the orbit was selected. The process of manufacturing the PMMA implant involved the routine steps of fabricating an ocular prosthesis, that is, impression with an alginate, wax modeling, and mould making, converting into PMMA and final trimming, buffing, and polishing to make the implant rest in the basin of the inferior orbital fissure. This implant was sterilized before insertion into the patients' orbit.

Surgery details

An inferior transconjunctival incision was taken with a radiofrequency device 2 mm below the lower border of the tarsus and the floor of the orbit was reached with blunt dissection. The periosteum was incised just within the orbital margin and reflected to expose the basin of the inferior orbital fissure. The customized orbital PMMA implant was placed inferotemporally, in the basin of the inferior orbital fissure, conforming to the predesigned shape of the floor of the orbit. The recentration of the pre-existing spherical implant was confirmed by palpating through the conjunctiva. Conjunctiva was closed and inferior fornix forming sutures were placed when necessary and possible. For patients with severe shortening of the fornix, a fornix formation suture with mucus membrane graft was performed 6 weeks later. A well-fitting conformer was placed and a suture tarsorrhaphy was performed for all the cases.

Statistical analysis

The data were arranged on an Excel spreadsheet. Relevant statistical analysis was done using MedCalc version 12.2.1.0. Continuous parametric data were reported as mean ± standard deviation, and nonparametric data were reported as median with range. Variables between comparative groups were compared using paired *t*-test for parametric distribution and Mann–Whitney *U* test for non-parametric distribution. A *P* value of <0.05 was assigned as statistically significant.

Results

Case 1

A 47-year-old gentleman complained of an ill fitting prosthesis with frequent loss of the prosthesis from the eye socket. On clinical examination, the medial caruncular portion of the prosthesis was elevated from the conjunctival surface [Fig. 3a]. The inferior fornix was shelved and the implant was palpable anterior to the inferior orbital rim with inferotemporal migration [Fig. 3b]. Volume loss was evident in terms of SSD and enophthalmos. CT scan of the orbit showed an 18-mm orbital implant, migrated into the extraconal space in the inferotemporal quadrant [Fig. 3c]. He had undergone two socket surgeries in the past including an enucleation with implant for a painful blind eye followed by fornix formation sutures for a shallow inferior fornix. Based on the above findings, a diagnosis of inferotemporal implant migration was made and a PSI was fabricated as described above. This was placed in the basin of the inferior orbital fissure to recenter the migrated orbital implant. The surgical steps were as discussed in methods. A customized ocular prosthesis (COP) remained stable and central thereafter over his follow-up of 2 years. He underwent a ptosis surgery for mild anophthalmic ptosis after 18 months [Fig. 3d]. The spherical orbital implant was maintained in the central position over his entire follow-up period [Fig. 3e]. Hertel's exophthalmometry on both sides was equal. Postoperative CT scan of the orbit showed the PSI in place with intraconal recentration of the spherical implant [Fig. 3f]. There was no reduction in prosthesis motility.

Case 2

A 16-year-old boy presented with a tilted and unstable custom ocular prosthesis. On examination, he had a decentred prosthesis with its inferior edge resting on the lower eyelid margin. There was shelving of the inferior fornix with inferotemporal migration of the orbital implant resulting in frequent loss of prosthesis from the eye socket. The implant was palpable anterior to the inferior orbital rim. There was no apparent conjunctival surface loss. Volume loss was evident in terms of grade IV SSD. CT scan of the orbit showed an 18-mm orbital implant migrated inferotemporal into the extraconal space. He had undergone three socket surgeries in the past starting with an evisceration with implant for a painful blind eye followed by implant exchange twice with fornix formation sutures for inferotemporal implant migration and forniceal shelving. Owing to recurrent implant migration, we anticipated fibrosis in the orbit and hence did not consider an implant exchange. The patient refused a DFG after explaining about the donor site morbidity. Hence, we placed a PSI in the inferotemporal orbit that would push the migrated implant centrally. The postoperative course was uneventful and both the implants remained centered over 36 months of follow-up. There was no reduction in seen in the motility of the COP after PSI placement [Fig. 4]. This was the pilot case treated in this series.

Case 3

A 25-year-old gentleman presented to us with an unstable prosthesis on the right side. He was diagnosed to have right eye secondary glaucoma with ciliary staphyloma at the age of 8 years for which he underwent an enucleation with 18-mm PMMA implant. Six years later, he developed post-enucleation socket syndrome with a shallow of inferior fornix. He was operated for fornix formation over three sittings in the postoperative period over the next 11 years; however, he had recurrent shortening of the fornix. On examination, there was lower eyelid laxity with shallow inferior fornix and a grade 2 SSD. The implant was migrated in the inferotemporal quadrant and palpable anterior to the inferior orbital rim. He underwent a PSI placement in the inferotemporal quadrant. This was followed by a fornix formation suture with mucus membrane graft for surface expansion. A COP was fabricated and dispensed 6 weeks thereafter. Over the next 20 months, both the implants remained stable and so did the inferior forniceal depth. There was a posterior movement of the spherical implant in the *z*-axis along with its centration in the orbit following the placement of PSI [Fig. 5].

Case 4

A 24-year-old gentleman presented to us with complaint of frequent loss of the prosthesis from the eye socket. He had

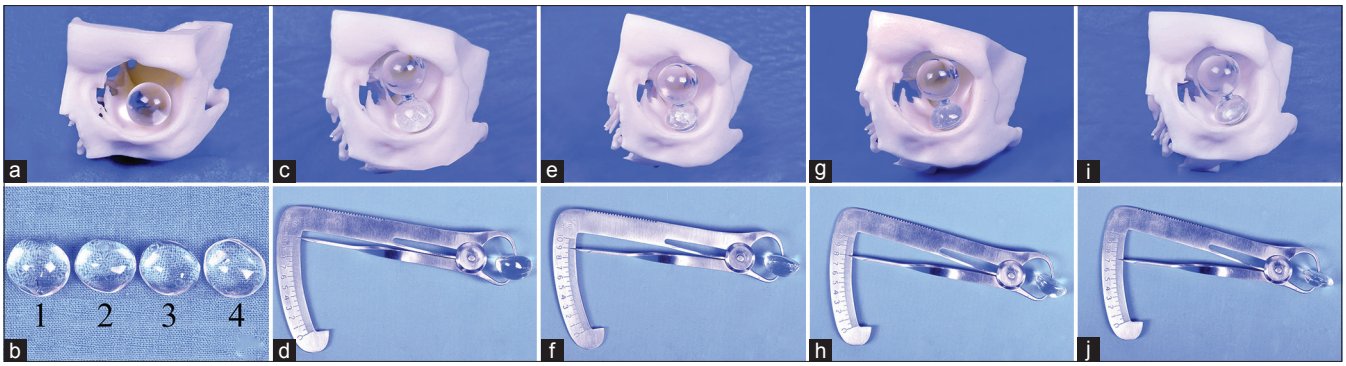

Figure 2: Deciding the height of patient-specific implant (PSI). (a) Placing the migrated orbital implant (diameter known from radiography) into the orbit in the migrated position, (b) four PSIs fabricated for this patient with diameters of 7, 8, 9, and 10 mm each, (c) 10-mm height PSI producing an excessive migration of the spherical implant toward the roof, (d) thickness of the 10-mm PSI being demonstrated with a caliper, (e) 9-mm height PSI producing an excessive migration of the spherical implant toward the roof, (f) thickness of the 9-mm PSI being demonstrated with a caliper, (g) 8-mm height PSI producing an excessive migration of the spherical implant toward the roof, (h) thickness of the 8-mm PSI being demonstrated with a caliper, (i) 7-mm height PSI producing an adequate migration of the spherical implant toward the roof, and (j) thickness of the 7-mm PSI being demonstrated with a caliper

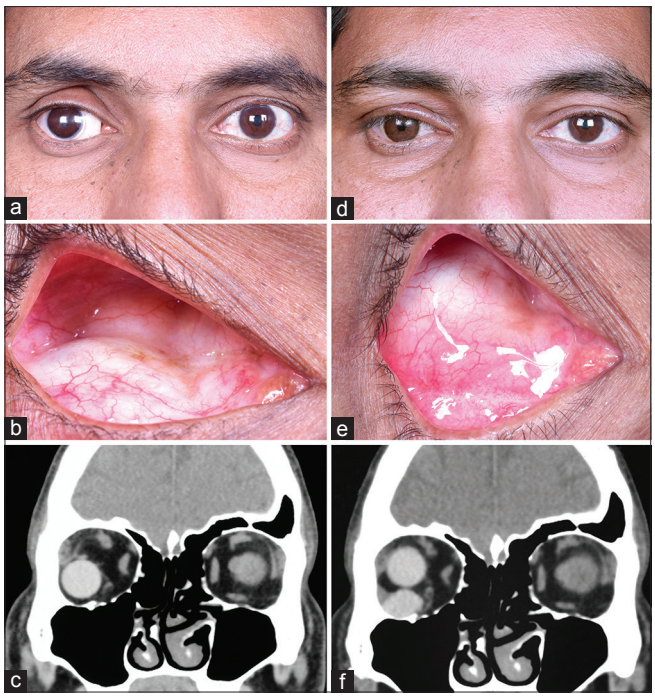

Figure 3: Pre- and postoperative pictures of case 1 treated with patient-specific implant. (a–c) Preoperative photographs, (d and e) postoperative photographs. (a) Preoperative appearance of the right side with an unstable prosthesis, (b) preoperative appearance of the right socket with an inferotemporal implant migration, (c) preoperative computed tomography scan with spherical implant migrated outside the intraconal space into the inferotemporal orbit, (d) postoperative appearance of the right side with a well-fitting prosthesis and a reduction in pretarsal shown on the right side following ptosis correction, (e) postoperative socket photograph showing a central implant, and (f) postoperative computed tomography scan showing a patient-specific implant pushing the migrated implant centrally

undergone right eye enucleation with a 16-mm implant for retinoblastoma at the age of 4 years. He was diagnosed to have inferotemporal implant migration with a shallow inferior fornix at the 3-month postoperative visit. Two years later, he underwent

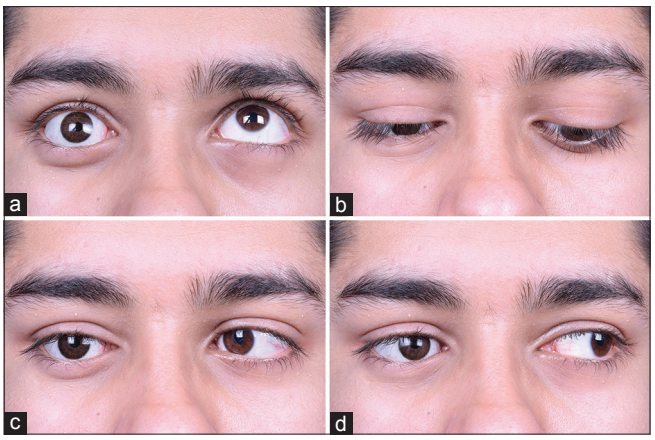

Figure 4: Motility of the prosthesis following patient-specific implant placement in patient 2. (a) Motility in upgaze, (b) motility in downgaze, (c) motility in right gaze, and (d) motility in left gaze

fornix formation sutures for the right side; however, the inferior fornix remained shallow in the postoperative period. He then underwent a PSI placement along with a fornix formation suture and over a follow-up period of 17 months, there were no complications noted. The postoperative scan revealed a posterior movement of the spherical implant in the *z*-axis along with its centration in the orbit following placement of PSI.

Case 5

A 43-year-old lady presented to us with complaints of frequent fall of the prosthetic eye from the left eye socket since the past 4 years. She had undergone an evisceration for panophthalmitis followed by secondary implant for volume augmentation 10 years ago. On examination, she had a sunken appearance of the prosthesis with a grade IV SSD and a 4-mm enophthalmos on the left side. There was inferotemporal implant migration with a shallow fornix. She underwent a PSI placement that helped center the migrated spherical implant. The fornix deepened after PSI placement. However, the SSD persisted for which she had a filler injection. Over a follow-up period of 15 months there

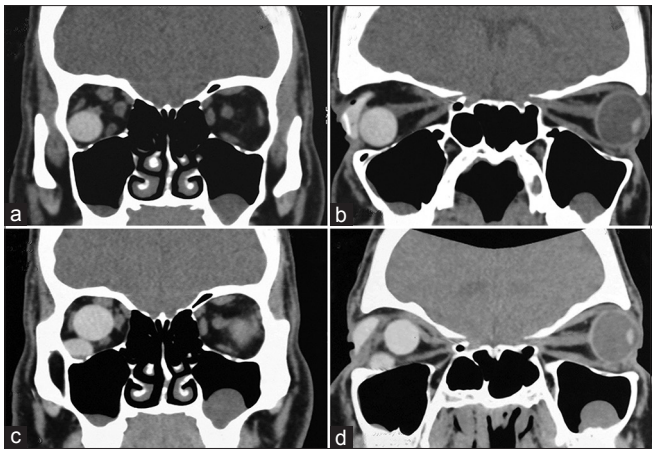

Figure 5: The direction of centration of the spherical implant in the orbit with placement of patient-specific implant in patient 3. (a and b) Preoperative computed tomography scan, (c and d) postoperative computed tomography scan, (a) preoperative computed tomography scan in the coronal cut showing an inferotemporal migration of the implant, and (b) preoperative computed tomography scan in the saggital cut. Note the position of the implant along the floor with relationship to inferior orbital rim, (c) postoperative computed tomography scan in the coronal view showing a centration of the implant in the *xy*-axis and (d) postoperative computed tomography scan in the saggital view. Note the posterior shift of the spherical implant in the orbit away from the inferior orbital rim due to the push by patient-specific implant

were no complications noted with either implants. The fornix remained deep thereafter.

Case 6

A 3-year-old boy was referred to us following enucleation with PMMA implant (18 mm) for retinoblastoma. On examination, there was a shallow inferior fornix and an inferotemporal implant migration. The implant was palpable anterior to the inferior orbital rim. The child was unable to retain a COP in the eye socket. A PSI was implanted into the basin of the inferior orbital fissure to recenter the implant. He underwent a Fornix formation suture (FFS) with mucus membrane grafting to deepen the fornix after 6 weeks. Over a follow-up period of 12 months, no complications were noted.

The baseline demographics, pre- and postoperative socket findings, and the results of surgery are as described in Table 1. None of the six patients developed complications of the spherical or PSI over a mean of 21-month follow-up. Three patients underwent a simultaneous inferior fornix formation suture for a shelved inferior fornix. Two patients underwent subsequent fornix formation suture and mucus membrane graft for grade 1 contracted socket with shallow inferior fornix. One patient required a levator reattachment for anophthalmic ptosis and one patient had persistent severe SSD for which hyaluronic acid gel filler was injected into the brow fat. The mean pre- and postoperative enophthalmos was 2.33 ± 0.81 and 0.5 ± 0.83 mm, respectively (P = 0.14). The mean preoperative SSD was grade 2 and postoperatively grade 0 (P = 0.1). The mean pre- and postoperative COP weights were 2.7 ± 1.25 and 2.2 ± 0.88 g, respectively (P = 0.37). The mean pre- and postoperative COP thickness was 7.16 ± 2.99 and 6.33 ± 1.21, respectively (P = 0.47). The mean PSI implant weight was 2.66 ± 0.53 g. There was no reduction in ocular motility post surgery with PSI [Fig. 4]. The average patient score of satisfaction with the final prosthetic outcome was 9 on 10.

Discussion

This study highlights that recentration of inferotemporal spherical implant migration post enucleation can be successfully treated by placing a second PSI in the quadrant of migration, thus pushing the migrated implant into the intraconal space. 3D printing facilitates this process by providing a mould of the orbit for the fabrication of PSI. The exact contour of the base of the PSI can be fabricated using the patient's printed orbit as a mould. This reduces the chances of further implant complications such as migration, exposure, and extrusion of PSI. Implant exchange is not a viable option for a migrated non-porous spherical orbital implant, possibly due to disturbances in the orbital compartments, intermuscular septae, and fibrosis within the orbit. The inferotemporal location of the PSI bypasses these orbital factors that hinder implant centration. To the best of our knowledge, this is a novel, minimally invasive application of 3D printing technology in ophthalmic plastic surgery with promising results.

A spherical orbital implant frequently tends to migrate anterior to the inferior orbital rim and hence shallows the fornix. A second implant placed in the basin of the IOF is crafted in such a way that it is dome-shaped. The dome of the second implant actually pushes the spherical implant posteriorly along the *z*-axis along with centration in the *xy*-axis of the orbit as shown in Fig. 5. This posterior displacement of the spherical implant is the most important contribution of this technique in our opinion. This also allows the fornix to remain formed over a longer period of time.

Non-porous spherical orbital implants suffer a higher rate of implant migration compared with their porous counterparts especially in the setting of enucleation.[13,14] However, in the absence of pegging, a porous implant does not provide additional motility compared with a non-porous implant.[1,15] Hence, surveys from the United States, the United Kingdom, and Asia Pacific have shown that a significant proportion of surgeons prefer to place a non-porous implant following socket surgery.[16,17] While the non-porous implant offers an excellent and comparable outcome to its porous counterpart, one of the important disadvantages is implant migration since it is devoid of fibrovascular tissue ingrowth into the implant.[1]

Implant migration has been poorly studied in literature. Kronish *et al*. analyzed the changes in orbital blood flow and circulatory dynamics of the socket tissues and atrophy of the orbital fat occurring after enucleation as two theoretical mechanisms that result in the development of implant complications in an animal model.[18,19] They concluded that circulation dynamics and blood flow to orbital tissues do not change after enucleation. In addition, there was no atrophy of the orbital fat following enucleation. Based on their investigations, they propose that the pathophysiologic basis of the problems associated with anophthalmos is a disturbance in the spatial architecture and interrelationships of the multiple tissue components of the orbit, not a change in the orbital blood flow or development of fat atrophy. Similar results were found by another independent research group in Brazil.[20] Tao *et al*. reported a series of five patients treated with Osmed hydrogel

Table 1: Baseline demographics, pre- and postoperative socket findings, and patient satisfaction scores

Serial number	Eye	Age (years)	Spherical implant diameter (mm)	Preoperative COP weight[†] (gms)	Postoperative COP weight (gms)	Preoperative SSD[@]	Postoperative SSD
1	OD	47	18	2.70	2.49	Grade 1	Grade 1
2	OD	17	18	3.70	1.75	Grade 4	Grade 0
3	OD	25	18	4.11	1.99	Grade 2	Grade 0
4	OD	21	16	3.30	3.8	Grade 4	Grade 4
5	OS	45	18	1.20	1.20	Grade 0	Grade 0
6	OD	3	18	1.20	2.00	Grade 2	Grade 0
Mean±SD		26.3±16.95	17.66±0.81	2.7±1.25	2.2±0.88	Grade 2	Grade 0

Preoperative enophthalmos[#] (mm)	Postoperative enophthalmos (mm)	Preoperative COP thickness[§] (mm)	Postoperative COP thickness (mm)	PSI implant weight (gms)	Follow-up duration (months)	Patient satisfaction with the prosthesis (0-10)*
2	0	7	8	2.50	24	9
2	0	10	7	2.70	36	9.5
2	1	11	6	2.00	20	8
2	2	7	7	3.5	17	9
4	0	5	5	3.00	15	8
2	0	3	5	2.30	12	9
2.33±0.81	0.5±0.83	7.16±2.99	6.33±1.21	2.66±0.53	20.66±8.57	9

COP: Custom ocular prosthesis, SSD: Superior sulcus deformity, PSI: Patient-specific implant, SD: Standard deviation, OD: Right eye

[†]Prosthesis weight was measured on the same weighing scale for all the patients; [@]Superior sulcus deformity was graded as Grade 0–Grade 4, Grade 0 representing no sulcus deformity, Grade I representing barely visible superior sulcus deformity, Grade II representing definite medial superior sulcus deformity, Grade III representing medial ± central superior sulcus deformity and Grade IV representing a total superior sulcus deformity spanning from medial to lateral superior sulcus; [#]Enophthalmos was measured with Hertel's exophthalmometry over the prosthetic eye; [§]COP thickness was measured by the same caliper for all the patients and was measured from the apex of the cornea to the back surface of the prosthesis at the central point of the pupil; *The patients on a scale of 0-10 (0 representing the worst and 10 representing the best) graded their satisfaction with the final aesthetic outcome

spheres in the management of congenital clinical anophthalmos and concluded that all the five implants had a similar path of movement in the inferotemporal quadrant of the orbit.[4,21] They suspected that the rapid rate of implant expansion contributes to migration in the path of least resistance and that inferolateral migration is conceivable, considering gravitational forces and orbital geometry. In our opinion, the cause of implant migration seems to be disturbances in the Koornneef's septa that are present between the extraocular muscles and divide the orbit into its extra and intraconal spaces.[22-25] Once these septa are disturbed or damaged during socket surgery, the chances that an implant may migrate increase. This is specifically true in case of enucleation where there is more disturbance of the orbital anatomy versus evisceration. Four of the six patients in our series suffered implant migration following enucleation.

With this background knowledge, that it is the disturbance in the orbital anatomy and possible fibrosis that increases the risk of non-porous implant migration, it is most certain that an implant exchange with non-porous implant will not help in recentering a migrated spherical orbital implant. The use of a porous implant for implant exchange may be an alternative; however, a theoretical risk of the porous implant migrating before the commencement of fibrovascular ingrowth exists. In addition, the cost of a porous implant is approximately $ 350 versus that of a PMMA implant which is approximately $ 5. The cost difference itself may be prohibitive to convince the patient for surgery.[26] This leaves us with the option of DFG. However, the requirement for a second site incision and the higher rate of graft necrosis in repeat socket surgeries makes this procedure an unattractive choice.[7,27]

3D printing and rapid prototyping have been used in ophthalmic plastic surgery for the correction of complex orbito-zygomatic fractures and in creation of PSIs for volume augmentation in the orbit.[28-30] 3D printing and computer-assisted techniques allow for the creation of patients' orbit *in vitro* using freely available softwares such as CURA. This orbital model serves as a mould for fabrication of PSI. The orbit can be printed with readily available and inexpensive range of materials in plastic. The cost of 3D printers can range from INR 10,000 to several lakhs; however, there is a large scope to outsource this facility. Since in our case the implant is not directly printed and the role of the printer is to provide a mould of the orbit for fabrication of PSI, we have not included the cost of the printer. The software used for the generation of 3D model and sending the STL file to the printer was an open access one. The cost of the printed orbit was INR 7000. The cost of fabrication of PSI was INR 150.

In most patients, a posterior movement of the implant in the *z*-axis was demonstrable on postoperative CT scan. In our opinion, this allows the fornix to remain deep in the postoperative period, as the implant is not occupying the space in the inferotemporal fornix. Four of the six patients in our cohort had prior attempts to deepen the inferior fornix, which failed. In our opinion, this was due to the migrated implant sitting in the inferotemporal fornix, with a part of the implant palpable anterior to the inferior orbital rim, and hence not allowing the fornix to deepen.

The limitations of this study include a small patient cohort and a relatively shorter duration of follow-up. The cost-effectiveness of the treatment has been calculated by taking into account only the cost of 3D printing and the cost of the printer has not been factored into. The 3D printed model gives the exact contour of the base of PSI but does not provide the ideal height of PSI, and indirect techniques as described in Fig. 2 need to be deployed to check the ideal height. The procedure does involve placement of a second implant in the orbit and this increases the risk of implant-related complications. The mean follow-up duration of 21 months may be a limitation; however, no complications related to both the implants were seen over this follow-up duration. We do recommend a longer follow-up of these cases.

Conclusion

PSI fabrication using 3D printing offers a novel and cost-effective way to center orbital implants in patients with implant migration. This is especially true for patients who have associated volume loss and in patients where a part of the implant is palpable anterior to the inferior orbital rim. Preoperative 3D printing enables us to determine the exact shape of PSI, which in our belief reduces further complications of orbital implant placement. Most importantly, the inferotemporal location of PSI ensures prevention of further implant migration.

Declaration of patient consent

The authors certify that they have obtained all appropriate patient consent forms. In the form the patient(s) has/have given his/her/their consent for his/her/their images and other clinical information to be reported in the journal. The patients understand that their names and initials will not be published and due efforts will be made to conceal their identity, but anonymity cannot be guaranteed.

Acknowledgement

We are grateful to Mr. Chary and Mr. Naresh for making of photo collages. We acknowledge the help provided by Mr. Choudhary and Mr. Goud in fabrication of prosthesis and patient-specific implants.

Financial support and sponsorship

This study was funded by The Hyderabad Eye Research Foundation.

Conflicts of interest

There are no conflicts of interest.

References

1. Custer PL, Kennedy RH, Woog JJ, Kaltreider SA, Meyer DR. Orbital implants in enucleation surgery: A report by the American Academy of Ophthalmology. Ophthalmology 2003;110:2054-61.
2. Custer PL, Trinkaus KM. Porous implant exposure: Incidence, management, and morbidity. Ophthalmic Plast Reconstr Surg 2007;23:1-7.
3. Sagoo MS, Rose GE. Mechanisms and treatment of extruding intraconal implants: Socket aging and tissue restitution (the "Cactus syndrome"). Arch Ophthalmol 2007;125:1616-20.
4. Tao JP, LeBoyer RM, Hetzler K, Ng JD, Nunery WR. Inferolateral migration of hydrogel orbital implants in microphthalmia. Ophthalmic Plast Reconstr Surg 2010;26:14-7.
5. Sundelin KC, Dafgård Kopp EM. Complications associated with secondary orbital implantations. Acta Ophthalmol 2015;93:679-83.
6. Quaranta-Leoni FM, Moretti C, Sposato S, Nardoni S, Lambiase A, Bonini S, *et al.* Management of porous orbital implants requiring explantation: A clinical and histopathological study. Ophthalmic Plast Reconstr Surg 2014;30:132-6.

7. Nentwich MM, Schebitz-Walter K, Hirneiss C, Hintschich C. Dermis fat grafts as primary and secondary orbital implants. Orbit 2014;33:33-8.
8. Dave TV, Gaur G, Chowdary N, Joshi D. Customized 3D printing: A novel approach to migrated orbital implant. Saudi J Ophthalmol 2018. doi: 10.1016/j.sjopt.2018.03.003.
9. Dave TV, Ezeanosike E, Basu S, Ali MJ, Kaliki S, Naik MN. Effect of optic nerve disinsertion during evisceration on nonporous implant migration: A comparative case series and a review of literature. Ophthalmic Plast Reconstr Surg 2018;34:336-41.
10. Kaltreider SA, Lucarelli MJ. A simple algorithm for selection of implant size for enucleation and evisceration: A prospective study. Ophthalmic Plast Reconstr Surg 2002;18:336-41.
11. Ushijima S, Ukimura O, Okihara K, Mizutani Y, Kawauchi A, Miki T. Visual analog scale questionnaire to assess quality of life specific to each symptom of the international prostate symptom score. J Urol 2006;176:665-71.
12. Brokelman RB, Haverkamp D, van Loon C, Hol A, van Kampen A, Veth R. The validation of the visual analogue scale for patient satisfaction after total hip arthroplasty. Eur Orthop Traumatol 2012;3:101-5.
13. Migliori ME. Enucleation versus evisceration. Curr Opin Ophthalmol 2002;13:298-302.
14. Custer PL. Enucleation: Past, present, and future. Ophthalmic Plast Reconstr Surg 2000;16:316-21.
15. Tari AS, Malihi M, Kasaee A, Tabatabaie SZ, Hamzedust K, Musavi MF, *et al.* Enucleation with hydroxyapatite implantation versus evisceration plus scleral quadrisection and alloplastic implantation. Ophthalmic Plast Reconstr Surg 2009;25:130-3.
16. Su GW, Yen MT. Current trends in managing the anophthalmic socket after primary enucleation and evisceration. Ophthalmic Plast Reconstr Surg 2004;20:274-80.
17. Viswanathan P, Sagoo MS, Olver JM. UK national survey of enucleation, evisceration and orbital implant trends. Br J Ophthalmol 2007;91:616-9.
18. Kronish JW, Gonnering RS, Dortzbach RK, Rankin JH, Reid DL, Phernetton TM, *et al.* The pathophysiology of the anophthalmic socket. Part I. Analysis of orbital blood flow. Ophthalmic Plast Reconstr Surg 1990;6:77-87.
19. Kronish JW, Gonnering RS, Dortzbach RK, Rankin JH, Reid DL, Phernetton TM, *et al.* The pathophysiology of the anophthalmic socket. Part II. Analysis of orbital fat. Ophthalmic Plast Reconstr Surg 1990;6:88-95.
20. Shiratori CA, Schellin SA, Marques ME, Padovani CR, Padovani CR. Orbital fat evaluation after enucleation and evisceration in rabbits. Arq Bras Oftalmol 2005;68:631-3.
21. Schittkowski MP. Re: "Inferolateral migration of hydrogel orbital implants in microphthalmia". Ophthalmic Plast Reconstr Surg 2010;26:503.
22. Ettl AR, Salomonowitz E, Koornneef L. Magnetic resonance imaging of the orbit: Basic principles and anatomy. Orbit 2000;19:211-37.
23. Ettl A, Koornneef L, Daxer A, Kramer J. High-resolution magnetic resonance imaging of the orbital connective tissue system. Ophthalmic Plast Reconstr Surg 1998;14:323-7.
24. Ettl A, Kramer J, Daxer A, Koornneef L. High-resolution magnetic resonance imaging of the normal extraocular musculature. Eye (Lond) 1997;11 (Pt 6):793-7.
25. Koornneef L. Orbital septa: Anatomy and function. Ophthalmology 1979;86:876-80.
26. Ho VW, Hussain RN, Czanner G, Sen J, Heimann H, Damato BE, *et al.* Porous versus nonporous orbital implants after enucleation for uveal melanoma: A randomized study. Ophthalmic Plast Reconstr Surg 2017;33:452-8.
27. Bosniak SL. Complications of dermis-fat orbital implantation. Adv Ophthalmic Plast Reconstr Surg 1990;8:170-81.
28. Callahan AB, Campbell AA, Petris C, Kazim M. Low-cost 3D printing orbital implant templates in secondary orbital reconstructions. Ophthalmic Plast Reconstr Surg 2017;33:376-80.
29. Scawn RL, Foster A, Lee BW, Kikkawa DO, Korn BS. Customised 3D printing: An innovative training tool for the next generation of orbital surgeons. Orbit 2015;34:216-9.
30. Baumann A, Sinko K, Dorner G. Late reconstruction of the orbit with patient-specific implants using computer-aided planning and navigation. J Oral Maxillofac Surg 2015;73:S101-6.